Wall-less ion-counting nanodosimetry applied to protons

G. Garty[1, *], S. Shchemelinin[1], A. Breskin[1], R. Chechik[1], I.Orion[1], G.P. Guedes [1], R. Schulte[2], V. Bashkirov[2] and B. Grosswendt[3]

[1] The Weizmann Institute of Science, 76100 Rehovot, Israel
[2] Loma Linda University Medical Center, Loma Linda, CA 92354, USA
[3] PTB, D-38116, Braunschweig, Germany

Abstract:

A wall-less ion-counting nanodosimeter, conceived for precise ionization-cluster measurements in an accelerator environment, is described. The technique provides an accurate means for counting single radiation-induced ions, in dilute gas models of condensed matter. The sensitive volume dimensions, a few tissue-equivalent nm in diameter by a few tens of nm, are tunable by a proper choice of the gas pressure and electric fields; nanometric subsections can be electronically selected. We present detailed ion-cluster distributions with protons of 7.15, 13.6 and 19.3 MeV, in biologically relevant DNA-like sensitive volumes of low-pressure propane. Experimental results are compared to model simulations.

Introduction

Based on the current understanding of radiobiology, the most relevant target for radiation damage in tissue is a cylinder of 2.3nm diameter and 16nm length, corresponding to a 50 base pair segment of DNA[(1,2)]. Clustered damage, which is believed to be produced by correlated ionization clusters, deposited by radiation in such volumes, has a potential of inducing damage, which may escape the enzymatic repair mechanisms in the cell. Therefore, these ionization clusters are most relevant for assessing the radiation quality. The stochastic process of ionization in such small volumes cannot be investigated with conventional microdosimetric techniques; these are suitable for providing useful information about the ionization deposition within volumes on the cell scale, but are not expected to provide an adequate description of the nanometric clustering of ionization on the DNA scale.

We have proposed to study these phenomena by measuring the amount and spatial correlations of ionizations induced in a low-density gas model of condensed matter[(3,4,5)]. We have developed a unique nanodosimeter (ND), based on the idea of the detection of single ions[(6)] induced by radiation in a cylindrical wall-less sensitive volume (SV) of low density gas. The latter simulates a volume of condensed matter with a diameter of a few nanometers and a length of several tens of nanometers. The technique permits measuring ionization clusters deposited within the entire SV or in nanometric fractions of its length, permitting also the correlation of fragments of the ionization cluster formed at different distances from the particle track[(5)]. The tunable-size SV is designed to be wall-less, resulting in a genuine evaluation of ion distributions, omitting possible secondary wall effects. This feature is of prime importance in view of the small size of the SV and of the small energy deposits involved. It is important to note that the ion-counting nanodosimeter described in this work does not require any special properties from the operating gas (such as scintillation or charge multiplication). We present here for the first time, in a concise form, the results of precise measurements of ionization clusters induced by low-energy (7.15, 13.6 and 19.3 MeV) protons in propane. A more extended description of the instrumentation, methods and results will be presented elsewhere[(7)].

* Corresponding author : guy.garty@weizmann.ac.il
fax : 972-8-934 2611

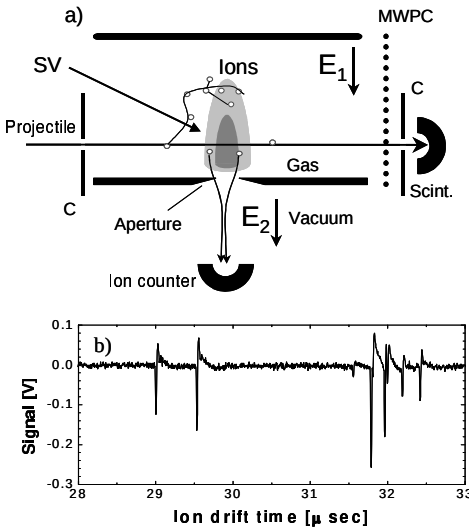

Figure 1: a) A schematic diagram of the ion counting nanodosimeter and its trigger system. See text. **b)** An example of a pulse- trail induced by 4.3 MeV alpha particles; each 20 nsec-wide pulse is induced by a single accelerated ion.

Experimental procedures

The structure of the ion-counting nanodosimeter is shown schematically in figure 1. Positive ions deposited by ionizing particles within the SV are extracted under an electric field, through a 1mm circular aperture, from the gas into vacuum; they are accelerated by high-voltage focusing electrodes onto an ion detector, where they are individually recorded and counted with an efficiency above 90%[8]. A double differential pumping system maintains a pressure gradient between the ionization volume (1.33 mbar) and the detection volume (10^{-5} mbar).

The nanodosimeter is filled with a dilute gas, expanding the *linear scale* of interaction by a factor equal to the *density ratio*[9]. Using 1.33 mbar of propane, at room temperature, one mm in gas is equivalent to 2.36 nm in unit-density tissue. Single-ion pulses, within an ionization cluster induced by a given projectile, are counted. Such data is collected from many individual projectiles, providing the full statistical distribution of the ionization cluster-sizes induced in a given sensitive volume, for any charged particle beam.

In accelerator experiments, a particle beam, scattered by a thin foil and collimated by a 1mm circular collimator (C), traverses the ND gas volume enclosed between two 2.5 μm thick Mylar windows, and ionizes the dilute gas (see figure1). All particles are detected by a multiwire proportional chamber (MWPC) placed downstream from the ND volume. Non-scattered particles are post-selected, off-line by a collimated scintillation detector (Scint.). In our conditions, the ND permits operation at a beam flux of up to a few thousands of particles per second.

An example of a typical pulse-trail, with a sequence of pulses corresponding to the individual ions induced in the gas, is shown in figure 1b. In addition to the number of ions, it contains information on the arrival time of each ion to the counter, which correlates to its deposition location along the SV (the drift axis). This important additional information may be used to measure the ionization density across the particle's path (ionization profile), and to subdivide the SV length into smaller subsections, a few nanometers long. The latter may serve as a base for *experimental track-nanodosimetry,* providing a way of correlating ionization clusters deposited by a single projectile at different distance from the track, as discussed above. This is possible, because the information on the initial ion deposition location is rather well preserved, due to the relatively small diffusion in gas, limiting the attainable resolution to a few nm in our conditions.

The nanodosimeter was irradiated by 7.15, 13.6 and 19.3 MeV protons at the Weizmann Institute of Science's Pelletron accelerator. In all cases the protons were collimated to a pencil beam of 1 mm diameter with a divergence of 0.5 milliradians; the beam was aligned to pass through a point located 15±0.2mm above the ion extraction aperture (see figure 1). The arrival times of the detected ion signals in an event, as well as the signal from the scintillator were recorded for every MWPC trigger, using a National Instruments PCI-6602 timer/counter DAQ board. The system was designed to suppress pile-up events, originating from projectiles arriving within the ion collection time of a previous event (about 80 microseconds). To ensure efficient pile-up rejection capability the MWPC, placed downstream from the ND, provides a trigger signal for every projectile crossing the sensitive volume, including those scattered within the beam-line and the ND; the scintillation detector, collimated to 1mm diameter, post-selects those projectiles that traverse the sensitive volume, without scattering, at the exact distance of 15 mm above the aperture. The absolute frequency of

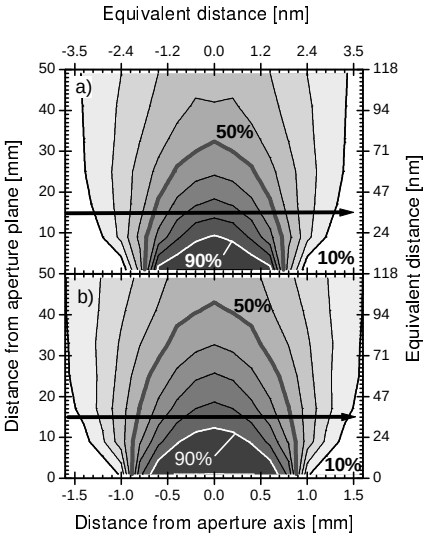

Figure 2: Monte Carlo- simulated maps of the ion extraction efficiency, defining the wall-less sensitive volume. Each contour line represents a change of 10% in the ion collection efficiency (the thick line is 50%). The arrow represents the location of the collimated beam in the present experiments. The bottom and left scales are real distances in gas, while the top and right scales provide the equivalent distances in tissue. The length of the SV presented in the text is measured along the SV axis, while the width is measured at the base. Figure a) corresponds to an electric field configuration: E_1 = 60V/cm, E_2=700V/cm and b) corresponds to E_1 = 60V/cm, E_2=1100V/cm.

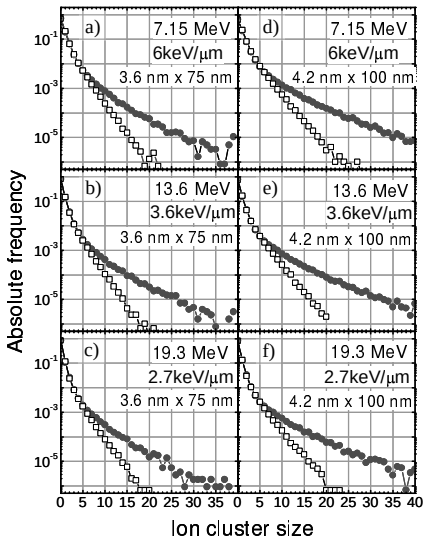

Figure 3: Experimental (full symbols) and simulation (hollow symbols) results of the ionization cluster- size distributions, induced in the two sensitive volumes shown in figure 2, by low-energy protons. The energies and corresponding LET values are indicated in the figure. Figures a-c correspond to the map shown in figure 2a; figures d-f correspond to the map shown in figure 2b. Note that the simulation and experimental result are in excellent agreement down to event frequencies below 10^{-3}.

generating an n-ion cluster is calculated after the rejection of possible pile-up events.

Calculated sensitive volume

The extraction efficiency of the ions through the aperture defines the size and shape of the wall-less sensitive volume, which was calculated, based on the electric field geometry in the ND system and on the measured transport parameters of the ions[5]. The SV is represented by a map of tapered, cylindrically symmetrical volume-contours, corresponding to equal ion extraction efficiencies, as seen in figure 2. The size of the sensitive volume, in the tissue-equivalent scale can be parameterized, for example, by the 50% ion extraction efficiency contour. The sensitive volume diameter is broader than the physical diameter of the aperture, due to penetration of electric fields from the acceleration electrodes, through the aperture, imposing some focusing. This effect allows an easy tuning of the sensitive volume, by modifying the electric fields. The two maps shown were calculated for the same drift field in the gas volume, with a different focusing field in the vicinity of the ion extraction aperture, resulting in different width and length of the sensitive volume. In the experiments reported here, this contour has a maximal diameter equivalent to 3.6 or 4.2 nm and a length equivalent to 75 or 100nm, respectively, in a tissue-equivalent scale. As detailed below, the length of the sensitive volume can be reduced, off line, by imposing ion arrival time cuts on the raw data.

It should be noted that the ion focusing in the vicinity of the extraction aperture is extremely sensitive to its exact configuration (diameter and thickness) and to the electric field on its vacuum (lower) side. As this focusing has a large impact on the size and shape of the sensitive volume, it could be a source of large uncertainty; experiments of direct mapping of the sensitive volume with high resolution tracking means are under preparation.

Results

Measured proton-induced nanodosimetric spectra

Figure 3 shows cluster-size distributions obtained with protons at different beam

Energy [MeV]	LET [keV/μm]	Average cluster size [ions]	Empty clusters [%]	Cluster frequency 2-5 ions [%]	Cluster frequency 6-10 ions [%]
3.6 nm x 75 nm sensitive volume					
19.3	2.3	0.25	85	4	0.34
13.6	3.6	0.33	80	5.7	0.47
7.15	6	0.56	69	10	0.88
4.2 nm x 100 nm sensitive volume					
19.3	2.3	0.33	81	5.1	0.53
13.6	3.6	0.44	76	7	0.71
7.15	6	0.74	63	13	1.3

Table 1: Nanodosimetric parameters extracted from the experimental data of figure 3. The average cluster size, and the frequencies at which clusters of various sizes occur for protons with different LET values are provided for the two sensitive volumes depicted in figure 2.

energies, using the two wall-less sensitive volumes shown in figure 2. Due to the relatively low linear energy transfers (LET) (2.7 to 6 keV/μm) of protons, the large ionization clusters are rather rare, and more than 60% of all projectiles induced no ionizations at all. Our results, based on data collection of a few hours per energy and SV configuration, at an average beam rate of a few thousands of particles per second, provide absolute frequency (normalized to the total number of events) for correlated multiple-ionization events within a given sensitive volume, down to a frequency of 10^{-6}.

Table 1 shows examples of some nanodosimetric parameters that may be extracted from figure 3. While the average cluster size reflects the amount of energy deposited in our sensitive volume, we can easily obtain more detailed information regarding the absolute frequency of events having any cluster size. In particular, the absolute frequency of clusters of 2-5 ions or 6-10 ions may be useful within the framework of various biophysical models such as the two-compartment model[2] for predicting irreparable damage induced in DNA by various radiation fields.

Comparison with Monte-Carlo Simulations

The experimental results were compared with those of a Monte-Carlo simulations, based on experimental ionization cross sections of protons and on experimental electron interaction cross sections with regard to elastic scattering, excitation and ionization in propane[10,11]. The energy and angular distributions of secondary electrons set in motion by primary particles were determined in the framework of the HKS model[12]. The secondary electrons and higher-order electrons induced by successive ionizing interactions were then followed through the gas until their energy reached a value below the ionization threshold (11 eV). Finally, the calculated ion extraction efficiency maps (fig.2) were applied to obtain a full simulation of the measured cluster size spectra at the two sensitive volume configurations described above.

Results of the MC simulations are shown, with the measured data in figure 3. For the small clusters (up to 5 ions/projectile) there is a very good correspondence between the measurement and the simulation results, with a discrepancy of less than 10% in the measured frequency to obtain an n-ion cluster. For larger clusters, appearing at a level of 10^{-3}, we consistently measure higher frequencies than in the simulations. A possible explanation for this effect is the existence of residual charge multiplication in the gas volume. Electrons induced in the gas by the proton beam may gain sufficient energy to ionize the gas, inducing excess ions. This mechanism is currently under study and is the most reasonable explanation for the observed discrepancy. This effect can be avoided by cleaning out the electrons under a low field, followed by ion collection under a high pulsed field[5]. Other possible sources of systematic errors, arising from beam quality and distortions in the DAQ system are also under study.

Arrival time analysis

As we are recording the arrival time of each ion, it is possible to trace-back to its deposition distance within the gas volume. This permits to correlate the frequency of different-size ionization clusters with the

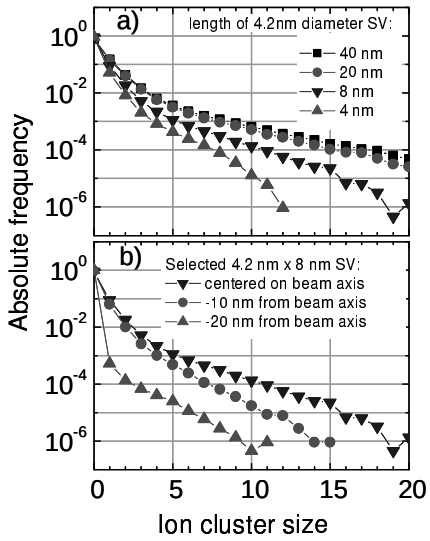

Figure 4: Experimental results of ionization cluster-size distributions, induced in slices of the sensitive volume shown in figure 2b (SV diameter: 4.2nm). These spectra were derived from the data in figure 3e, employing various ion arrival time windows. **a)** Centered on the beam axis and extending by 2, 4, 10 and 20 nm on both sides. **b)** 4.2nm diameter and 8nm long, centered on the beam axis and displaced towards the aperture plane by 10nm and 20nm.

distance from the beam and obtain information about beam ionization profile. Two examples are shown in figure 4. Figure 4a provides the cluster size distributions in a series of slices, selected from the sensitive volume shown in figure 2b. The slices, of ~4.2nm diameter extend 2, 4, 10 and 20nm on both sides of the beam axis. The 13.6 MeV proton beam is 1mm wide and passes 15mm (~ 40nm) above the aperture. This type of analysis can be used for evaluating ionization cluster distributions in different size sensitive volumes, as may be required by different biophysical models (e.g. see reference 2).

Figure 4b shows the distribution within a 4.2nm diameter and 8nm long sensitive volume selected at different distances from the beam axis: centered on the beam axis and displaced towards the aperture plane by 10nm and 20nm, respectively. This type of analysis may be useful in investigating the track structure.

As there is practically no difference between the 20nm long sensitive volume and the 40nm one (fig. 4a), it can be estimated that most of the ionizations occur within a distance of less than 20nm from the center of a 13.6MeV proton track. A more complete and systematic analysis, taking into account the variation in ion extraction efficiency along the sensitive volume axis and ion diffusion effects is in course.

Conclusions

We have constructed an ion-counting nanodosimeter, capable of measuring ionization clusters in very small gas volumes, representing nanometric scales of condensed matter. We have measured cluster-size distributions induced by low-LET protons in 3.6 nm x75 nm and 4.2 nm x100 nm tissue-equivalent gas volumes; the target gas was 1.33 mbar of propane. A second nanodosimeter is currently operating at the Loma-Linda University proton synchrotron, under higher energy (40-250MeV) proton beams.

Here we reported on ionization measurements with low LET protons. We are currently completing a series of measurements with alpha-particles and carbon ions, in the LET range of 100-600keV/μm; these data will be reported separately[7].

Although our device is not yet fully optimized, and some systematic errors are still under study, the presented data demonstrate the strength of ion-counting nanodosimetry. Unlike conventional microdosimetry, designed to assess radiation effects at the cell scale, the proposed technique permits measuring ionization clustering at the scale of a relevant segment of the DNA molecule. Compared to other nanodosimetric techniques[13,14], the ion-counting nanodosimeter provides a wall-less sensitive volume, the capability of subdividing it into small subsections for ionization-correlation measurements and the possibility of operating at high particle repetition rates with any gas. Our technique permits evaluating the absolute frequency of very large and very rare clusters (in this work down to the 10^{-6} level) with reasonable accuracy. It is expected that these large ionization clusters are the key to quantifying irreparable radiation damage to DNA.

Acknowledgements

The authors are indebted to Prof. M. Hass, Dr. O. Heber, Y. Shachar and G. Assaf, for their assistance with the accelerator experiments and to M. Klin for his technical assistance. S. Shchemelinin is supported by the state of Israel, the Ministry of Absorption and the Center for Absorption of Scientists. A.

Breskin is the W. P. Reuther Professor of Research in the peaceful uses of Atomic Energy

This work was partially supported by the National Medical Technology Testbed Inc. (NMTB) under the U.S. Department of the Army Medical Research Acquisition Activity, Cooperative Agreement Number DAMD17-97—2-7016 and by the MINERVA Foundation. The views, opinions and/or findings contained in this report are those of the authors and should not be construed as a position, policy, decision or endorsement of the US Federal Government and NMTB.

References

1. Nikjoo H. and Charlton D.E., *Calculation of range distributions of damage to DNA by high- and low-LET radiations*. In: A.F. Fuciarelli, J. D. Zimbrick (Eds.), Radiation damage in DNA: structure/function relationships at early times. Batell Press, Columbus, pp. 29-41, 1995.

2. Schulte R., Bashkirov V., Shchemelinin S., Garty G., Chechik R., Breskin A., *Modeling of radiation action based on nanodosimetric event spectra*. Physica Medica, Vol. XVII, Suppl. 1, (2001),177-180.

3. Shchemelinin S., Breskin A., Chechik R., Pansky A., and Colautti P. *A nanodosimeter based on single ion counting*. In: Microdosimetry - An interdisciplinary approach. Goodhead D., O'Neel P. & Menzel H. (Eds.), The Royal Society of Chemistry (Cambridge), pp 375-378 , 1997.

4. Shchemelinin S., Breskin A., Chechik R., Pansky A., Colauti P., Conte V., De Nardo L., and Tornielli G. *Ionization measurements in small gas samples by single ion counting*. Nucl. Instr. & Meth. **A368**, (1996) 859-861.

5. Shchemelinin S., Breskin A., Chechik R., Colautti P., and Schulte R.W. *First ionization cluster measurements on the DNA scale in a wall-less sensitive volume*. Radiat. Prot. Dosim, **82,(1999)** 43-50.

6. Chmelewski D., Parmentier N. and Le Grand J. *Dispositif experimental en vue d'etudes dosimetriques au niveau du nanometre* Proceedings of the fourth symposium on microdosimetry, EUR 5122 d-e-f, CEC, Luxemburg, 1973, p.869

7. Garty G., Shchemelinin S., Breskin A. Chechik R., Orion I., Schulte R., Bashkirov V. and Grosswendt B., In beam operation of an ion-counting nanodosimeter, *In Preparation*

8. Shchemelinin S., Pszona S., Garty G., Breskin A., and Chechik R. *The absolute detection efficiency of vacuum electron multipliers to keV protons and Ar^+ ions*. Nucl. Instr. & Meth.**A438**, (1999) 447-451.

9. Waker A.J., *Principles of experimental microdosimetery*. Rad. Prot. Dos. 61,(1995), 297-308

10. Grosswendt B. and Baek W.Y. *Basic Physical Data in Organic Gases*. In: Radiation Quality Assessment Based on Physical Radiation Interaction at Nanometer Level, ed. P. Colautti, LNL-INFN Report 161 (2000),5-26.

11. De Nardo, L., Conte, V., Baek, W. Y., Grosswendt, B., Colautti, P. andTornielli, G. *Measurements and Calculations of Ionisation Cluster Distributions in 20 nm Size Site*, LNL-INFN Report 175 (2001).

12. ICRU. Secondary Electron Spectra from Charged Particle Interactions. ICRU Report 55 (International Commission on Radiation Units and Measurements, Bethesda, MD, 20814, USA) (1996).

13. Pszona S., Kula J. and Marjanska S., *A new method for measuring ion clusters produced by charged particles in nanometre track sections of DNA size*. Nucl. Instrum.and Meth. A447 (2000) 601-607.

14. De Nardo L., Alkaa A., Khamphan C., Conte V. Colautti P., Dona G., Segur P. and Torinieli G., *A single-electron counter for track nanodosimetry*. LNL-INFN reprot 147 (2001)